F. Maggi, S. Dossi, C. Paravan, L.T. De Luca, M. Liljedahl
Activated Aluminum Powders for Space Propulsion
Powder Technology, Vol. 270, 2015, p. 46-52
doi:10.1016/j.powtec.2014.09.048

Activated aluminum powders for space propulsion

Filippo Maggi[a,1,*], Stefano Dossi[a,1], Christian Paravan[a,1], Luigi T. DeLuca[a,1], Mattias Liljedahl[b,2]

[a] *Politecnico di Milano, 34, via La Masa, 20156 Milan, Italy*
[b] *Swedish Defence Research Agency, FOI, SE-14725 Tumba, Sweden*

Abstract

Aluminum powders are commonly used in solid propellants to enhance the performance of space propulsion systems. During combustion, a fraction of the fuel metal particles, which emerge from the bulk, tends to merge into aggregates. These structures eventually leave the combustion surface in the shape of partially molten agglomerates which can reach the size of hundreds of microns. These condensed combustion products partake in nozzle expansion and hinder the delivered specific impulse of the rocket unit. The enhancement of original particle reactivity improves combustion quality and may reduce sensibly agglomerate size and relevant losses.

More reactive aluminum fuel can be obtained by activation of micron-sized powders, without resorting to the use of nano-metals. One of the methods consists of a chemical treatment with a processing solution which alters the standard oxide layer at the surface of the particles. Such modifications grant lower ignition temperature and faster propellant burning rates

*Corresponding author, Tel. +390223998287
Email addresses: filippo.maggi@polimi.it (Filippo Maggi), stefano.dossi@mail.polimi.it (Stefano Dossi), christian.paravan@polimi.it (Christian Paravan), luigi.deluca@polimi.it (Luigi T. DeLuca), mattias.liljedahl@foi.se (Mattias Liljedahl)
[1]Department of Aerospace Science and Technology, Space Propulsion Laboratory (SPLab)
[2]Department of Energetic Materials

but deplete a fraction of the active metal content, as a result of the chemical reaction.

The present paper compares the features of three batches of aluminum particles which were treated with fluorine-based activating solutions of different concentration. The batches were supplied in the frame of HISP FP7 European Project. The characterization focused on physical, chemical and thermal properties, looking at the reactivity of the samples and at the alterations introduced by the chemical processing. Finally, activated aluminum batches were tested in lab-scale propellants, monitoring the variation of ballistic properties with respect to a reference formulation.

Keywords: aluminum particles, chemical activation, reactivity, solid propellant, metal fuel

---

Nomenclature

Acronyms

BET Brunauer-Emmett-Teller

DTA Differential thermal analysis

ESD Electro Static Discharge

FCC face-centered cubic

SEM Scanning electron microscopy

TGA Thermal gravimetric analysis

TMD Theoretical mean density

XPS X-ray photoelectron spectroscopy

XRD X-ray diffraction

Greek symbols

α Degree of transformation

Δx Variation of x

ρ Density, g/cm^3

Roman symbols

C_{Al} Active metal fraction

$D_{4,3}$ Mass-mean diameter

m Mass, kg

r_b Burning rate, mm/s

p Pressure, bar

p Propellant

Subscripts and superscripts

in Initial condition

zK Ref. to the temperature of z Kelvin

1. Introduction

Gravimetric and volumetric specific impulse of solid rocket motors can be enhanced by using energetic additives [1–3]. Among the others, Aluminum has been adopted in solid space propulsion for decades, in the shape of micrometric metal powders, thanks to its appealing energetic content (30 kJ/g), stability in time, non-toxicity, and relatively low cost. Typical particle sizes range from 5 to 50 microns [4, 5].

A fraction of the metal embedded in a propellant tends to aggregate and agglomerate during combustion. Drops of molten aluminum with an oxide cap leave the burning surface [6, 7]. These condensed combustion products generate a multiphase flow which expands through the nozzle. Performance losses are the order of 2-5% of the ideal specific impulse, depending on size and amount of the particulate [8, 9]. In this respect, the improvement of metal fuel ignition and combustion is envisaged in order to obtain finer agglomerates, or no agglomeration at all [3, 10].

Aluminum particles are covered by a natural oxide layer, as soon as they get in contact with oxygen-containing environments. This passivation shell represents a strong shield against further degradation by the atmospheric oxygen. At the same time, it represents an obstacle to reactivity. Under burning conditions, ignition occurs when the passivating alumina shell fails, enabling fast oxidation of the metal core. The melting temperature of the oxide layer (about 2300 K) is necessary to trigger the combustion, when par-

ticle size is in the order of tens of micrometers. Nevertheless, values as low as 1300 K were recorded in presence of some kinds of active media (namely, combustion products inside rocket core flow) [11]. Ignition temperature is below 900-1000 K, for nanometric powders. Particles take advantage of sample specific surface and active coating layers, if any [12].

Literature data agree on the fact that the use of nanometric particles in propellants improves ignition and combustion properties, preventing from large agglomerates [13–15]. However, the reduction of particle size introduces some drawbacks. The relative amount of aluminum oxide with respect to the total particle mass can become relevant in the nanometric range, since the thickness of the oxide layer (about 2.5-3 nm) does not scale with particle size [16]. The consequent reduction of the active metal content depresses the available oxidation enthalpy and, in turn, propulsion performance (namely, ideal specific impulse). Moreover, mixing and casting of a propellant containing nanometric ingredients may represent a technological issue due to high viscosity, reduced pot life, ESD (Electro Static Discharge) and impact hazards as well as cost of the manufactured compound [17].

Specific activation processes can be performed on metal particles to improve ignition and combustion properties, without decreasing the diameter to the sub-micrometric range. Mechanical ball milling, coating with properly chosen metals, or chemical weakening of the external oxide layer represent some examples. Mechanical milling operates a modification of particle morphology by high-energy impact with processing spheres. Synthesis of amorphous powders, structure change, production of metal-ceramics, or inclusions of reactants (metal oxides or fluorides) can be achieved [18–21]. Coating of particles through deposition of metals can improve ignition and combustion properties, such as for magnesium-coated boron [22–24]. The weakening of

the oxide shell can be pursued through chemical treatment. A complex fluoride acts as solvent for alumina, lowering the melting point of the protective aluminum oxide layer as well as accelerating the diffusion of gaseous oxidizer towards the metal core [25, 26].

The present paper focuses on the effects produced by a chemical activation process. Aluminum powder treated with three different activating solutions of varying concentrations are considered. Physical, chemical, and thermal characterizations, typically applied to nanometric powders, are performed to evaluate reactivity and final quality of the material [13, 27]. Comparison with original non-treated micron-sized Al as well as with some representative literature data for nanoaluminum and microaluminum is carried out. Combustion analysis of solid propellant samples containing activated powders are presented.

2. Experimental

Three batches of activated aluminum powders (A-Al01, A-Al02 and A-Al03) have been produced, following a procedure similar to the one described by Hahma [25, 28]. The initial aluminum was Valimet H3 powder (batch 07-8002). The producer rated 99.0% of minimum metal content and particle size of 4.5 μm [29]. The activation process was accomplished by a fluorine-based solution, whose concentration was varied to modify the strength of the treatment. The batch A-Al01 was assumed as reference for the processed family. The concentration of the solution was the half for A-Al02 and 1.5 times for A-Al03. Powder processing was conducted at FOI (Swedish Defence Research Agency), as part of the HISP (High Performance Solid Propellants for In-Space Propulsion) FP7 project.

The characterization tests of the powders comprised laser granulometry,

SEM, XRD, XPS, evaluation of the active metal content, and TGA/DTA scans. Different composite solid rocket propellants were compounded and their ballistic properties were experimentally tested. Moreover, the contraction of ideal performance, following the depletion of metallic aluminum during activation, was monitored by means of thermochemical analysis [30].

2.1. Physical characterization

SEM micrographs, reported in Figure 1, show a comparison between Valimet H3 and all activated batches. Particles appear mainly spherical. The external surface is smooth for the original powders and rough for the processed ones. The activated particles also feature some irregular deposits, not present in the original material, whose size seems to follow the concentration of the activating solution. Namely, the spots covering the A-Al03 surface reach the size of about 100 nm, whereas smaller dimensions are observed in the other cases. A precise estimation is difficult to supply.

[Figure 1 about here.]

Particle size was measured by means of a Malvern Mastersizer 2000 using air dispersion with Scirocco dry unit. Mass-mean diameter $D_{4,3}$, span of the distribution, and evaluation for the specific surface, derived from geometric considerations, are reported in Table 1. Valimet H3 and activated powders do not demonstrate appreciable differences. All particles have a comparable mass-weighted diameter ranging between 5.1 and 5.5 μm and similar distribution shape and relevant span. For all activated powders, mean particle diameter grows few hundreds of nanometers. Representative distribution plots are reported in Figure 2 for A-Al01 and H3. Reduction of the particles

Table 1: Parameters for physical particle characterization. Literature data of ALEX^{TM} and ASD-4 are reported for reference. Specific surface areas derive from both BET method and particle size analysis.

Id.	H3 (baseline)	A-Al01	A-Al02	A-Al03	ALEX^{TM} [a]	ASD-4 [b]
Activating solution relative concentration	0	1.0	0.5	1.5	-	-
$D_{4,3}, \mu m$	5.1	5.5	5.4	5.5	0.1	9.0
Span	1.78	1.66	1.68	1.64	-	-
Specific surface area, m^2/g (BET)	1.2	2.6	2.2	3.3	11.8	0.38
Specific surface area, m^2/g (particle size)	2.5	2.1	2.1	2.0	-	-

[a] Ref.[31]
[b] Ref.[32]

finer than 1 μm diameter, presumably lost during the chemical process, is observed.

[Figure 2 about here.]

A more representative evaluation of the powder specific surface is accomplished using the BET technique [33]. The estimation is based on the quantity of adsorbed inert gas on the surface of a sample. The result depends on both geometric aspect of the particles and on the peculiarities of the surface (namely, roughness) [35]. According to Barret, particle characterization is accomplished when size, shape and finish are addressed [36]. Bouwman and co-authors stress on the fact that surface roughness and shape are difficult to define since their distinction derives, in general, from considerations on characteristic dimensions which, in turn, depend on the observation scale [37]. In this respect, the specific surface measurement using the BET technique is a condensed and comprehensive value, which includes all contributions. This kind of analysis has been adopted in the past to characterize fine and ultra-fine metal powders, also for energetic purposes. The measurement was considered a reliable index of reactivity [10, 34].

The resulting trend among the tested batches is correlated with the concentration of the activating solution. The specific surface from BET analysis is incremented by the activation process. The reference A-Al01 doubles the specific surface, if compared to the original H3 supply. A-Al02 features the lowest BET improvement while A-Al03 has the highest value, respectively less-than-double and almost three times the value of H3 batch. Laser granulometry assessed that the mean diameter of the particles was almost unchanged by the chemical processing so the variation of specific surface is attributed to porosity increment. These results are in agreement with SEM observations.

2.2. Chemical characterization

The quantification of the metallic aluminum in the powder, after the chemical processing, is performed by hydrolysis. The moles of H_2 developed by samples, once in contact with water, are monitored in time till stabilization is obtained. A solution of NaOH (10% concentration by mass) is used to dissolve the external oxide shell and facilitate the process. Following a standard volumetric method [38], the assumed stoichiometric reaction is

$$Al + 3\,H_2O \rightarrow Al(OH)_3 + (3/2)H_2 \uparrow + \text{heat} \tag{1}$$

The moles of reacted metal from the evolved hydrogen can be determined.

This chemical activation process has the unwelcome effect to deplete part of the aluminum from the powder. The metal content of the initial powder batch was quantified in more than 98%. Tests on activated samples showed a consistent contraction of the Al content. The decrement was only in part dependent on the concentration of the activating solution. For the powder which underwent the strongest activation (A-Al03), only 90% of particle mass was estimated to be active aluminum. For A-Al01 and A-Al02, the fraction was around 93%.

X-ray analyses were also performed on the samples. For all the powders, XRD identified the presence of aluminum only, in face-centered cubic (FCC) crystalline form, regardless of the activation. The diffraction pattern for the A-Al01 sample is reported in Figure 3. The result indicates that the superficial chemical treatment did not generate detectable quantities of crystalline compounds. The samples were further analyzed with XPS, for identification of surface elemental composition. Different atomic species were introduced by the activation process, such as fluorine, present with a 13.0% atomic concentration, boron 3.0%, manganese 2.1% and potassium 1.5%. Among

the identified atomic species there was also carbon 5.4%, oxidized aluminum 17.0% and oxygen 58.0%.

[Figure 3 about here.]

2.3. Thermogravimetric analysis

The effects of enhanced particle reactivity on intensive oxidation onset and other related parameters were analyzed by means of TGA/DTA in air at ambient pressure. Scans were performed on 10 mg samples with 10 K/min heating rate, up to 1273 K (1000°C). As representatives, the scans of A-Al01 and of H3 baseline are reported in Figure 4, using the same scales on the axes for immediate comparison. Overall results are reported in Table 2. The DTA trace of A-Al01 shows an oxidation peak, overlapped to the melting of the aluminum core, in proximity of 933 K. The reaction is forerun by an initial exothermic release. From the analysis of peak positions for different activated materials, it appears that stronger activation does not anticipate the oxidation onset towards lower temperatures. The baseline H3 powder did not show proofs of fast oxidation in the same range of temperature. This behavior is in line with past experimental findings, available in the open literature. The ignition of standard micrometric powders is size-dependent and, for the range of interest, fast oxidation is expected to occur above 1273 K (1000°C). [39].

The degree of transformation α can be quantified via TGA data. The value of α represents the fraction of the actual aluminum content in the initial sample mass m_{in} which turned into its oxide. The measure is based on the recorded mass increment Δm_{TGA} and on the initial active metal fraction C_{Al} of the respective batch, quantified with the volumetric method described before. The value of α is computed using equation 2, which derives from simple

considerations about respective molar masses. Exclusive and stoichiometric conversion of Al into Al_2O_3 is assumed.

$$\alpha\left(Al \rightarrow Al_2O_3\right) = \frac{\Delta m_{\mathrm{TGA}}}{0.889} \frac{1}{m_{\mathrm{in}}\, C_{\mathrm{Al}}} \tag{2}$$

In consideration of TGA results, the degree of transformation was evaluated at three reference temperatures and, namely, α_{933K} at 933 K for aluminum melting, α_{973K} at 973 K once the Al melting peak is over, and α_{1273K} at the final scanning temperature 1273 K. A correlation between activation strength and degree of metal oxidation was missing even though a general increment of the oxidized fraction was observed at the end of the test for activated powders.

When DTA/TGA traces for A-Al01 and H3 are compared (see Figure 4), a different rate of weight increment and, as consequence, of oxidation can be observed. The H3 sample progressively increased its mass during the whole TGA scan. Rather, A-Al01 showed an abrupt increment during the exothermic peak, indicating a fast oxidation reaction. However, most of the metal-oxide conversion occurred while the aluminum core was already in liquid state, meaning that metal consumption at particle ignition was rather limited.

[Figure 4 about here.]

2.4. Application in propellants

The influence of powder activation on solid propellant properties was assessed. Four aluminized formulations based on AP oxidizer and HTPB binder were produced, using different batches of metal fuel. The same nominal composition, reported in Table 3, was adopted for the comparison. Three

Table 2: Parameters for chemical and thermal particle characterization. ALEX^{TM} and ASD-4 properties, available from the literature, are reported for comparison.

Id.	H3 (baseline)	A-Al01	A-Al02	A-Al03	ALEX^{TM} [a]	ASD-4 [b]
Active metal, %	98.3 ± 0.7	93.9 ± 0.9	93.7 ± 0.5	90.5 ± 0.5	89	98.5
DTA oxidation peak, K	N.A.[c]	934 K	943 K	939 K	876	1093 (onset)
Δm_{TGA} at 1273 K, %	+39	+41	+52	+54	+ 66	-
α_{933K}, %	8	4	6	5	-	2.5
α_{973K}, %	15	25	17	12	-	-
α_{1273K}, %	44	49	62	67	82	41

[a] Ref.[31]
[b] Ref.[32]
[c] Out of the experimental range 298–1273 K

propellants were manufactured by using one of the activated aluminum powders while the baseline formulation contained the raw H3 non-activated metal fuel. The characterization activity consisted of the measurement of bulk density, porosity, and relevant ballistic data reduction.

[Table 1 about here.]

Propellant density ρ_p was assessed by means of buoyancy technique. Its difference $\Delta\rho_p$ from the corresponding ideal value (mainly due to porosity) was evaluated using the formula $\Delta\rho_p = (\rho_p - \rho_{id})/\rho_{TMD}$. Propellant combustion tests were carried out in a closed combustion chamber, equipped with automatic pressure control system, in a range between 5 to 40 bar. Burning rate was assessed through optical technique using the SPLab proprietary software *Hydra*. The ensemble of results is reported in Table 4 while graphic comparison of burning rate curves is available in Figure 5.

[Figure 5 about here.]

[Table 2 about here.]

The use of activated metal fuels improved ballistic properties without introducing peculiar issues for propellant compounding and curing. Low level porosity was detected. The presence of the activation layer did not interact with curing processes or generated internal bubbling, at the mixing temperature of 36°C. These observations are in line with binder-fuel viscosity analyses recently published by the same research group [41]. For combustion tests, an increase of burning rate in the order of about +20%, with respect to the original non-activated powders, was observed. The increment was irrespective of the type of activation. Only minor differences were found among the tested lots. The r_b pressure dependence increased from non-activated to

activated metal fuels, but almost negligible differences were found. Ballistic data and relevant fittings are reported in Figure 5. The curves for P-A-Al01, P-A-Al02, and P-A-Al03 are overlapped, suggesting that the different concentration levels of the activating solution, tested in this framework, did not modify the combustion behavior of the propellants.

3. Discussion

The improvement of particle reactivity after the chemical activation process is registered by both the increment of the specific surface area (visible from BET analysis) and by the reduction of particle ignition temperature below 1273 K (observed in TGA/DTA traces). The improvement of the former reactivity parameter is caused by the generation of superficial roughness and is partially responsible of earlier particle ignition. However, the latter benefits also from oxide layer weakening. It is not possible to weight the different contributions, so far. In this respect, BET analysis records partially the significant role of the activating solution and the knowledge of the ignition temperature supplements the characterization.

The activation process caused only a surface modification of the raw material. XRD diffraction patterns did not reveal any in-depth modification of the crystalline structure, being the core still aluminum. XPS data identified several atomic species, laid by the chemical processing on a thin superficial layer.

It was verified that the amount of the active metal content was reduced even down to 90%. This latter aspect becomes crucial from a propulsion point of view. The enhancement of powder reactivity is performed with the purpose to reduce metal agglomeration during combustion and alleviate a fraction of the respective losses. However, such effort may not be worthwhile

if the performance gap due to active metal depletion approaches or even surmounts the potential gain for a better combustion and more efficient nozzle expansion. A quantification of such effect is reported in Figure 6. The ideal specific impulse for the reference propellant formulation, reported in Table 3, is computed through thermochemistry [40]. Expected contraction is about 1-2%, depending on activation strength and depleted metal. The reduction of two-phase flow losses cannot be assessed in this context , nevertheless the performance detriment is quantified in the open literature as 3-5%. That is, the improvement delivered by chemical activation of aluminum may be comparable to the negative effect caused by the contraction of the aluminum content. Careful evaluation of formulation ingredients is envisaged.

[Figure 6 about here.]

The TGA/DTA scans with low heating rate in oxidizing atmosphere (air in the present case) indicate the improvement of reactivity for activated aluminum particles at high temperature. Exothermic peaks are obtained about the melting point of aluminum. At the same time sample weight increment is promptly recorded. Such events are not visible for unprocessed H3 powder, in agreement with the literature. Available data suggest that fast oxidation rate should be achieved beyond 1273 K (experimental limit of this paper), for unprocessed powders having similar size and shape. In general, aluminum particle ignition, under combustion conditions, is triggered by the disruption of the oxide layer. This event occurs after the melting of the oxide shell (around 2300 K) for the micrometric range, or is caused by the expansion of the particle bulk for the nanometric size [39]. In this case, the exothermic peak and the consequent fast oxidation rate from DTA/TGA scans are overlapped with the melting of the aluminum. It is possible that the oxide shell, modified by the activation process, cracked at the melting of the bulk

and let the oxidation start. Metal consumption was limited by the size of the powder which did not grant enough specific surface area.

Activated aluminum powders result in intermediate properties, globally ranking their reactivity above comparable micron-sized aluminum, though still far from nano-sized particles. Tables 1 and 2 report some relevant literature data, along with results from the present paper. ALEX^{TM} refers to a nominally 100 nm aluminum produced by electrical explosion of wire (EEW). ASD-4 is a micrometric Russian product, comparable to H3 [31, 32]. Both powders are naturally passivated by air and are commercially available. Activated aluminum still have lower initial oxide content than the reference nanoaluminum but loses 5-8% of metal with respect to the initial ingredient. Resulting ideal specific impulse data are reported in Figure 6. The temperatures of the first oxidation peak for the A-Al family, detected by DTA/TGA, are significantly lower with respect to the behavior of micrometric ASD-4 sample and approach the features of the nanometric ALEX^{TM} powder. The degree of metal-oxide conversion at the end of the TGA scan increments for samples treated with stronger powder activation and is in the range 50-70%. Similarly, specific surface area (BET analysis) is incremented with respect to ASD-4 and H3, but the value is still 5 to 10 times lower than ALEX^{TM}. The burning rate analysis confirms a general +20%, after metal fuel processing. The reader should note that the benefit is five times less than the one obtained by using an ALEX^{TM} nano-sized aluminum [10].

Finally, experimental findings suggest that only minor differences exist among the activated powders from the reactivity viewpoint. The BET analysis identified about $\pm 0.5 m^2/g$ variation of specific surface area among the lots, which is rather limited for sensible repercussions. Similar assessments were highlighted by high-temperature tests. DTA/TGA powder oxidation

peaks are almost overlapped and the ballistic properties of P-A-Al propellants are very similar. The result is more meaningful if we consider that heating rates differ from each other in magnitude (10 K/min for DTA/TGA, and above 1000 K/s for propellant combustion).

4. Conclusions

Chemical activation of metal particles is a technique that fosters reactivity. The process is able to enhance ignition capability and increment the specific surface area through a solution of varying concentration. Both morphology and chemical composition of the external surface are modified by the chemical treatment, resulting in increased roughness and enriched with fluorine-based compounds. The metallic core is unaltered, but a consistent aluminum depletion reduces the active metal content of about 5-7%, for tested cases.

For the tested lots, the activation accomplished a general increment of particle reactivity. The specific surface area was more than doubled and DTA/TGA oxidation peak was anticipated at the melting of the aluminum core. However, the degree of metal-oxide conversion at ignition was slow. Most of the oxidation occurred at higher temperatures. Also the ballistic characterization confirmed the incremented reactivity. Uniform improvement of the burning rate was observed for all lots, showing negligible differences among tested activation strengths.

In general, powder properties obtained after chemical treatment are similar to the reactivity parameters of finer cuts, but are still far from the behavior of nano-sized ingredients. Increment in burning rate can be obtained when these advanced fuels are used in energetic materials. Also reduction of metal fuel agglomeration is envisaged but has to be proven with specific investiga-

tions. However, the potential benefits can be weakened or even impaired by the depletion of the active metal content, which is a direct consequence of the treatment.

5. Acknowledgements

The authors acknowledge the financial support of the European FP7 Project HISP (High performance solid propellants for In-Space Propulsion), Grant Agreement No. 262099. The authors wish to recognize and acknowledge the significant contribution of the Research Center for Non Conventional Energy, Eni Donegani Institute (Novara, Italy).

[1] N. Kubota. *Propellants and Explosives: Thermochemical Aspects of Combustion*. Wiley-VCH, second edition, 2007. ISBN 978-3-527-31424-9.

[2] F. Maggi, G. Gariani, L. Galfetti, and L. T. DeLuca. Theoretical analysis of hydrides in solid and hybrid rocket propulsion. *International Journal of Hydrogen Energy*, 37:1760–1769, 2012. doi: 10.1016/j.ijhydene.2011.10.018.

[3] L.T. DeLuca, L. Galfetti, F. Maggi, G. Colombo, A. Reina, S. Dossi, D. Consonni, and Brambilla. Innovative metallized formulations for solid rocket propulsion. *Chinese Journal of Energetic Materials*, 20(4): 465–474, 2012. doi: 10.3969/j.issn.1006-9941.2012.04.018.

[4] J. P. Sutton and O. Biblarz. *Rocket Propulsion Elements*. Wiley, New York, NY, USA, seventh edition, 2001. ISBN 0-471-32642-9.

[5] L. T. DeLuca. Burning of aluminized solid rocket propellants: from micrometric to nanometric fuel size. In P. Huang, Y. Huang, and S. Li, ed-

itors, *Proceedings of the 2007 International Autumn Seminar on Propellants, Explosives and Pyrotechnics*, volume VII of *Theory and Practice of Energetic Materials*, pages 277–289, 2007. ISBN: 978-7-03-020254-3.

[6] E. W. Price. Combustion of metallized propellants. In K. K. Kuo and M. Summerfield, editors, *Fundamental of Solid Propellant Combustion*, volume 90 of *Progress in Astronautics and Aeronautics Series*, pages 479–513. AIAA, New York, NY, USA, 1984. doi: 10.2514/5.9781600865671.0479.0513.

[7] F. Maggi, A. Bandera, L. Galfetti, L. T. DeLuca, and T. L. Jackson. Efficient solid rocket propulsion for access to space. *Acta Astronautica*, 66(11-12):1563–1573, 2010. doi: doi:10.1016/j.actaastro.2009.10.012.

[8] D. Reydellet. Performance of rocket motors with metallized propellants (AGARD PEP WG-17). AGARD AR-230, 1986.

[9] AA.VV. Solid rocket motor performance analysis and prediction. Technical Report SP-8039, NASA, May 1971.

[10] L. DeLuca, L. Galfetti, G. Colombo, F. Maggi, A. Bandera, V. A. Babuk, and V. P. Sinditskii. Microstructure effects in aluminized solid rocket propellants. *Journal of Propulsion and Power*, 26(4):724–733, 2010. doi: 10.2514/1.45262.

[11] P. F. Pokhil, A. F. Belyaev, Yu. V. Frolov, V. S. Logachev, and A. I. Korotkov. Combustion of metal powders in active media. Technical Report AD0769576, Defense Technical Information Center, 1972.

[12] Y. Huang, G. A. Risha, V. Yang, and R. A. Yetter. Effect of particle size on combustion of aluminum particle dust in air. *Combustion and Flame*, 156(1):5–13, 2009. doi: 10.1016/j.combustflame.2008.07.018.

[13] L. Galfetti, L. T. DeLuca, F. Severini, L. Meda, G. Marra, M. Marchetti, M. Regi, and S. Bellucci. Nanoparticles for solid rocket propulsion. *Journal of Physics: Condensed Matter*, 18(33):S1991–S2005, 2006. doi: 10.1088/0953-8984/18/33/S15.

[14] L. Galfetti, L. T. DeLuca, F. Severini, G. Colombo, L. Meda, and G. Marra. Pre and post-burning analysis of nano-aluminized solid rocket propellants. *Aerospace Science and Technology*, 11(1):26–32, 2007. doi: 10.1016/j.ast.2006.08.005.

[15] L. T. DeLuca, L. Galfetti, F. Severini, L. Meda, G. Marra, A. B. Vorozhtsov, V. S. Sedoi, and V. A. Babuk. Burning of nano-aluminized composite rocket propellants. *Combustion, Explosion and Shock Waves*, 41(6):680–692, 2005. doi: 10.1007/s10573-005-0080-5.

[16] E. L. Dreizin. Metal-based reactive nanomaterials. *Progress in Energy and Combustion Science*, 35:141–167, 2009. doi: 10.1016/j.pecs.2008.09.001.

[17] U. Teipel and U. Förter-Barth. Rheology of nano-scale aluminum suspensions. *Propellants, Explosives, Pyrotechnics*, 26(6):268–272, 2001. doi: 10.1002/1521-4087(200112)26:6<268::AID-PREP268>3.0.CO;2-L.

[18] C. C. Koch and J. D. Whittenberger. Mechanical milling/alloying of intermetallics. *Intermetallics*, 4(5):339–355, 1996. doi: 10.1016/0966-9795(96)00001-5.

[19] D. L. Zhang. Processing of advanced materials using high-energy mechanical milling. *Progress in Materials Science*, 49(3):537–560, 2004. doi: 10.1016/S0079-6425(03)00034-3.

[20] T. R. Sippel, S. F. Son, and L. J. Groven. Altering reactivity of aluminum with selective inclusion of polytetrafluoroethylene through mechanical activation. *Propellants, Explosives, Pyrotechnics*, 38(2):286–295, 2013. doi: 10.1002/prep.201200102.

[21] S. Dossi, F. Maggi, L. Facciolati, and L. T. DeLuca. Activation of micrometric aluminum – metal oxide mixtures by mechanical milling. In *5th European Conference on Aerospace Sciences (EUCASS), 1-5 July 2013, Munich (Germany)*, 2013.

[22] K. K. Pace, T. A. Jarymowycz, and V. Yang. Effect of magnesium-coated boron particles on burning characteristics of solid fuels in high-speed crossflows. *International Journal of Energetic Materials and Chemical Propulsion*, 2(1-6), 1993. doi: 10.1615/IntJEnergeticMaterialsChemProp.v2.i1-6.180.

[23] C. L. Yeh and K. K. Kuo. Ignition and combustion of boron particles. *Progress in Energy and Combustion Science*, 22(6):511–541, 1996. doi: 10.1016/S0360-1285(96)00012-3.

[24] L.T. DeLuca, E. Marchesi, M. Spreafico, A. Reina, F. Maggi, L. Rossettini, A. Bandera, G. Colombo, and B.M. Kosowski. Aggregation versus agglomeration in metallized solid rocket propellants. *International Journal of Energetic Materials and Chemical Propulsion*, 9(1), 2010. doi: 10.1615/IntJEnergeticMaterialsChemProp.v9.i1.60.

[25] A. Hahma, A. Gany, and K. Palovuori. Combustion of activated aluminum. *Combustion and flame*, 145(3):464–480, 2006. doi: 10.1016/j.combustflame.2006.01.003.

[26] E. Tornqvist. Method for the formation of malleable metal powders, 1967. US Paternt 3,301,494.

[27] T. J. Kondis. Monitoring activation of particulate aluminum, 1976. US Patent 3,986,674.

[28] A. Hahma. Method of improving the burn rate and ignitability of aluminium fuel particles and aluminium fuel so modified, June 10 2004. URL `http://patentscope.wipo.int/search/en/WO2004048295`. WO Patent WO/2004/048,295.

[29] VALIMET Inc.,Product Information Sheet, Aluminium Powder, 2011-07-06. URL `http://www.valimet.com/documents/pdffiles/alum_powder_specs.pdf`.

[30] S. Gordon and B. S. McBride. Computer program for calculation of complex chemical equilibrium compositions and applications. Technical Report RP-1311, NASA Reference Publication, 1994.

[31] A. Sossi, E. Duranti, M. Manzoni, C. Paravan, L. T. DeLuca, A. B. Vorozhtsov, M. I. Lerner, N. G. Rodkevich, A. A. Gromov, and N. Savin. Combustion of HTPB-based solid fuels loaded with coated nanoaluminum. *Combustion Science and Technology*, 185(1):17–36, Jan 2013. doi: 10.1080/00102202.2012.707261.

[32] A. P. Ilyin, A. Gromov, V. An, F. Faubert, C. de Izarra, A. Espagnacq, and L. Brunet. Characterization of aluminum powders I. parameters of reactivity of aluminum powders. *Propellants, Explosives, Pyrotechnics*, 27:361–364, 2002. doi: 10.1002/prep.200290006.

[33] H. Czichos, T. Saito, and L. Smith. *Springer handbook of materials*

measurement methods. Springer Verlag Berlin Heidelberg, 2006. doi: 10.1007/978-3-540-30300-8.

[34] A. Gromov, A. P. Ilyin, U. Förter-Barth, and U. Teipel. Characterization of aluminum powders: II. aluminum nanopowders passivated by non-inert coatings. *Propellants, Explosives, Pyrotechnics*, 31:401–409, 2006. doi: 10.1002/prep.200600055.

[35] T. Allen. *Particle Size Measurement: Volume 2: Surface Area and Pore Size Determination.* Powder Technology Series. Springer, 1996. ISBN 9780412753305.

[36] P. J. Barrett. The shape of rock particles, a critical review. *Sedimentology*, 27(3):291–303, 1980. doi: 10.1111/j.1365-3091.1980.tb01179.x

[37] A. M. Bouwman, J. C. Bosma, P. Vonk, J. H. A. Wesselingh, and H. W. Frijlink. Which shape factor(s) best describe granules? *Powder Technology*, 146(1):66–72, 2004. doi: 10.1016/j.powtec.2004.04.044

[38] A. P. Astankova, A. Yu. Godymchuk, A. A. Gromov, and A. P. Ilyin. The kinetics of self-heating in the reaction between aluminum nanopowder and liquid water. *Russian Journal of Physical Chemistry A*, 82(11): 1913–1920, 2008. doi: 10.1134/S0036024408110204.

[39] R. A. Yetter, G. A. Risha, and S. F. Son. Metal particle combustion and nanotechnology. *Proceedings of the Combustion Institute*, 32:1819–1838, 2009. doi: 10.1016/j.proci.2008.08.013.

[40] I. Glassman and R. F. Sawyer. The performance of chemical propellants. AGARDograph 129, 1970.

[41] F. Maggi. Curing viscosity of HTPB-based binder embedding micro- and nano-aluminum particles. *Propellants, Explosives, Pyrotechnics*, In press, 2014. doi: 10.1002/prep.201400010.

List of Figures

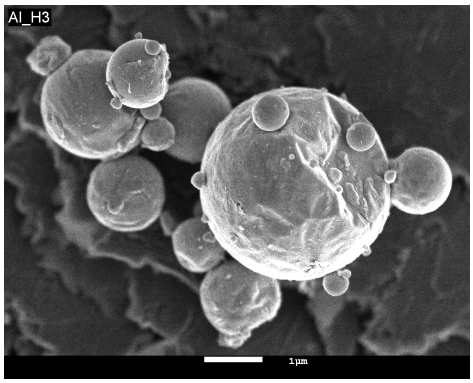

(a) Valimet H3

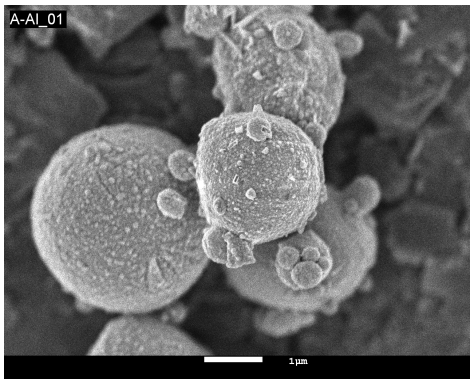

(b) A-Al01

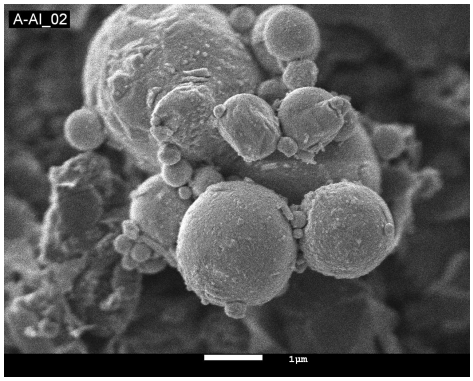

(c) A-Al02

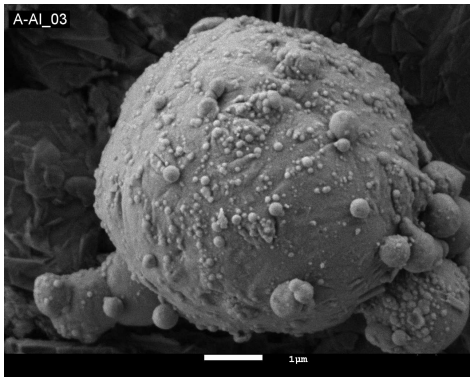

(d) A-Al03

Figure 1: SEM of virgin and activated aluminum powders. Magnification: 15,000x.

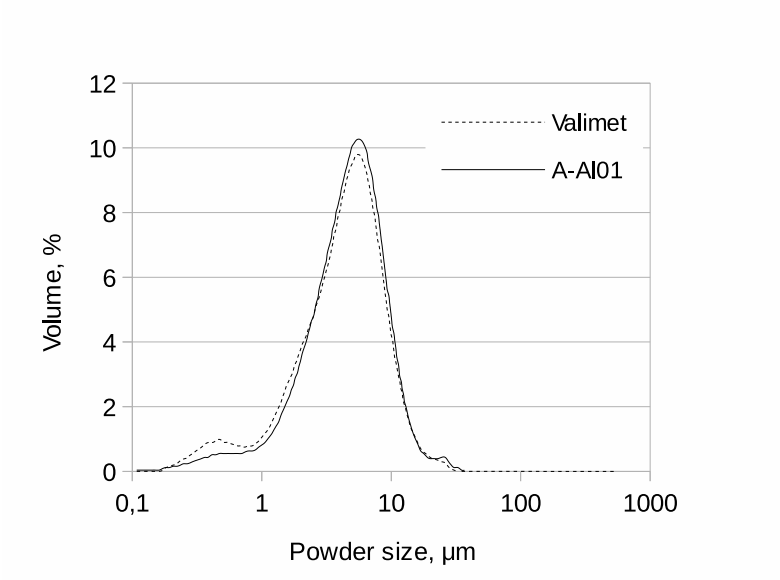

Figure 2: Granulometric distribution obtained by laser scattering of samples H3 and A-Al01.

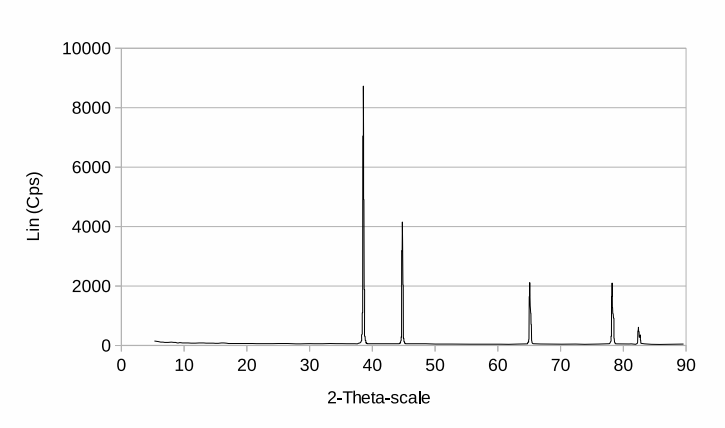

Figure 3: XRD spectrum of A-Al01 powder. Aluminum only is detected.

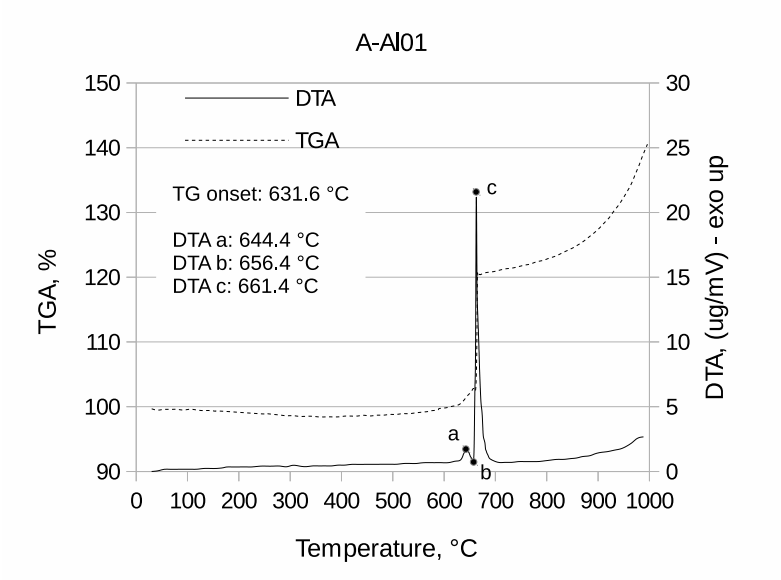

(a) A-Al01

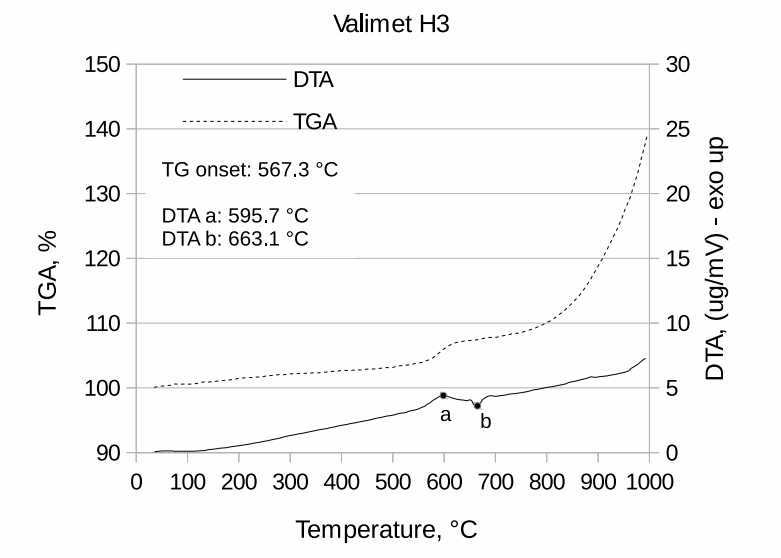

(b) Valimet H3

Figure 4: TGA/DTA analysis in air of H3 and A-Al01 powders. Sample weight 10 mg, temperature ramp 10 K/min.

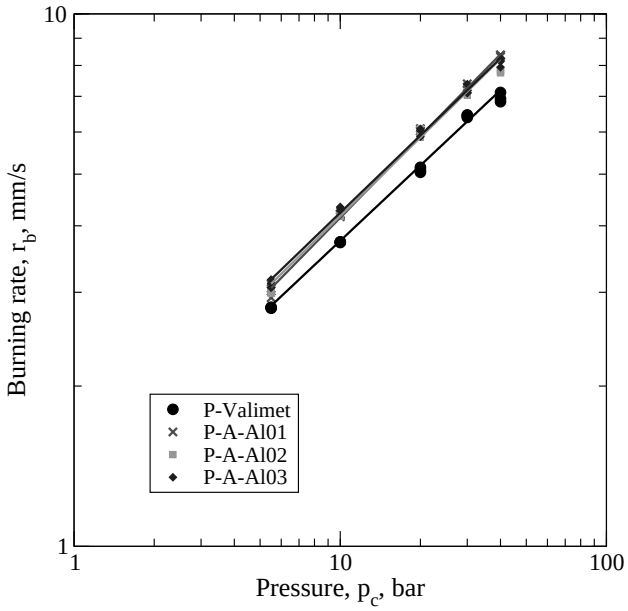

Figure 5: Steady burning rate vs. pressure of propellants embedding activated aluminum. Baseline formulation is included for comparison.

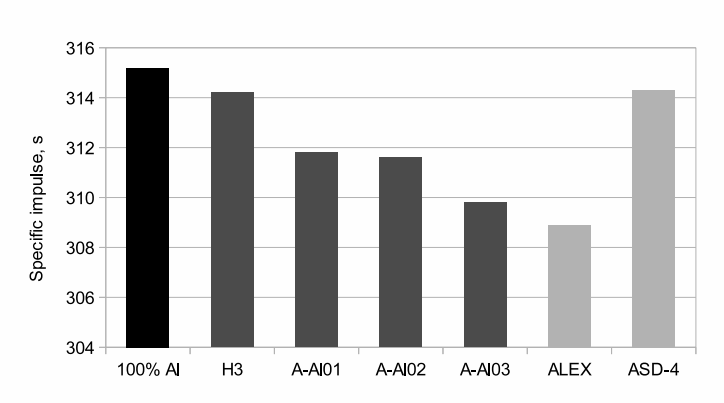

Figure 6: Ideal specific impulse for the formulation reported in Table 3. Computations are performed under the assumptions of 70 bar combustion pressure, expansion ratio of 40, discharge in vacuum [30].

List of Tables

Table 3: Nominal propellant composition for ballistic analysis ($\rho_{TMD} = 1.761 g/cm^3$). Mixing was performed at 36°C; a tin-based curing catalyst was used.

Ingredient	**Mass fraction**	**Notes**
Ammonium Perchlorate	58%	Coarse: 200 μm nominal
Ammonium Perchlorate	10%	Fine: 10 μm nominal
Metal fuel	18%	Aluminum: standard or activated
Binder	14%	HTPB-based

Table 4: Details of propellant characterization. Uncertainty was computed using a 95% confidence level.

Propellant	Powder	ρ_p, g/cm^3	$\Delta\rho_p$	Vieille's law
P-A-Al01	A-Al01	1.749	-0.7%	$r_b = (1.28 \pm 0.02)\, p^{(0.51\pm0.01)}$
P-A-Al02	A-Al02	1.727	-1.9%	$r_b = (1.35 \pm 0.04)\, p^{(0.49\pm0.01)}$
P-A-Al03	A-Al03	1.734	-1.6%	$r_b = (1.40 \pm 0.03)\, p^{(0.48\pm0.01)}$
P-Valimet	Valimet H3	1.749	-0.7%	$r_b = (1.27 \pm 0.03)\, p^{(0.47\pm0.01)}$